Available online at www.sciencedirect.com

SciVerse ScienceDirect

Energy Procedia 37 (2013) 550 – 559

Energy Procedia

GHGT-11

ZrO_2-Supported CuO Oxygen Carriers for Chemical-Looping with Oxygen Uncoupling (CLOU)

Mehdi Arjmand[a,*], Henrik Leion[a], Tobias Mattisson[b], Anders Lyngfelt[b]

[a]*Department of Chemical and Biological Engineering, Division of Environmental Inorganic Chemistry, Chalmers University of Technology, SE-412 96 Göteborg, Sweden*

[b]*Department of Energy and Environment, Division of Energy Technology, Chalmers University of Technology, SE-412 96 Göteborg, Sweden*

Abstract

The chemical-looping combustion (CLC) and chemical-looping with oxygen uncoupling (CLOU) processes are novel solutions for efficient combustion with inherent separation of carbon dioxide. In this work, oxygen carriers based on CuO supported by zirconia (ZrO_2) and stabilized by calcia (CaO), magnesia (MgO) and ceria (CeO_2) are investigated. The oxygen carriers were produced by freeze-granulation and calcined at 950 and 1050°C. Their chemical-looping performance was evaluated in a laboratory-scale fluidized-bed reactor at 900 and 925°C under cyclic oxidizing, inert (N_2) and reducing (CH_4) conditions. Five out of six oxygen carriers exhibited rapid release of oxygen in the inert environment (CLOU). Also, complete conversion of methane was obtained for three out of the six oxygen carriers. However, only in the case of MgO-stabilized ZrO_2 as support and calcined at 950°C, the oxygen carrier exhibited intact active CuO phase; agglomeration and particle fragmentation were also not observed. Thus, the use of this material could be suggested as a suitable oxygen carrier for the CLOU process.

Selection and/or peer-review under responsibility of GHGT

Keywords: CO_2-capture; chemical-looping combustion (CLC); chemical-looping with oxygen uncoupling (CLOU); oxygen carrier; copper-oxide; stabilized ZrO_2

1. Introduction

As suggested by the intergovernmental panel on climate control (IPCC), a 50-85% reduction in total CO_2 emission by 2050 is necessary to limit the anticipated global temperature rise to 2°C [1]. A number of alternative technologies have been proposed to mitigate the rising levels of carbon dioxide in the

* Corresponding author. Tel.: +46-31-772-2822; fax: +46-31-772-2853.
E-mail address: arjmand@chalmers.se.

1876-6102
Selection and/or peer-review under responsibility of GHGT
doi:10.1016/j.egypro.2013.05.141

atmosphere. Among these, carbon capture and storage (CCS) is considered promising. The chemical-looping combustion (CLC) process allows inherent separation of pure CO_2 from hydrocarbon combustion. In a CLC system, two reactors, a fuel reactor and an air reactor, are interconnected [2-4]. When fuel and air are introduced into the respective reactor, the following reactions occur

$$(2n+m)Me_xO_y + C_nH_{2m} \rightarrow (2n+m)Me_xO_{y-1} + nCO_2 + mH_2O \quad (1)$$

$$2Me_xO_{y-1} + O_2 \rightarrow 2Me_xO_y \quad (2)$$

Here Me_xO_y and Me_xO_{y-1} are the fully oxidized and reduced forms of an oxygen carrier. The scheme of the process is shown in Fig. 1. In case of complete conversion of the fuel, the exhaust stream from the fuel reactor consists of only CO_2 and H_2O, from which pure CO_2 could be obtained after condensation of water. The reduced form of the oxygen carrier, Me_xO_{y-1}, is then transferred to the air reactor where it is re-oxidized by air making it ready for the next cycle. The oxidation reaction is always exothermic while the reduction reaction can be exothermic or endothermic depending on the difference between the heat of oxidizing the fuel and reoxidizing the oxygen carrier [5]. However, the sum of the heat from reactions (1) and (2) is the same as for conventional combustion. Thus the CLC process does not entail any direct cost or energy penalty for CO_2 separation. CLC has been successfully demonstrated in a number of units of sizes up to 120 kW [6]. Overviews of current achievements in CLC are given by Lyngfelt [6, 7], Hossain and de Lasa [8], and Adanez et al. [9].

The reactivity of the oxygen carrier during oxidation and reduction and the ability to fully convert the fuel are among the most sought-after criteria. In addition, thermal stability, mechanical strength, fluidizability and resistance to attrition and agglomeration are important. In order to achieve this, the active phase (i.e. the reactive metal oxide) is often mixed with an inert support such as TiO_2, SiO_2, ZrO_2, Al_2O_3 or $MgAl_2O_4$ [8]. The CLC process can be used with gaseous, liquid or solid fuels. In the case of solid fuels, the char remaining after devolatilization is gasified in the presence of steam, producing CO and H_2 which can then react with the oxygen carrier. Alternatively, chemical-looping with oxygen uncoupling (CLOU) [10], could be used, where the char reacts directly with gaseous oxygen released from the oxygen carrier particles. In comparison to CLC, where the reduction of oxygen carrier and oxidation of the gaseous fuel generally occurs in a single step, an additional step is needed in CLOU for the release of gaseous oxygen from the carrier prior to conversion of the fuel according to

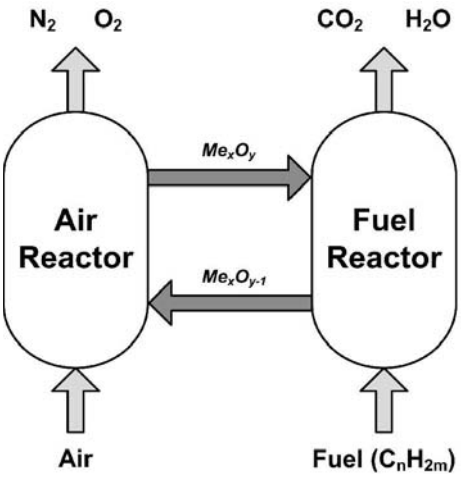

Fig. 1 Schematic of the Chemical-Looping Combustion (CLC) process

$$Me_xO_y \rightarrow Me_xO_{y-2} + O_2 \quad (3)$$

This is followed by the normal combustion of the fuel via

$$C_nH_{2m} + (n+m/2)O_2 \rightarrow nCO_2 + mH_2O \quad (4)$$

The reduced oxygen carrier is transferred to the air reactor for re-oxidation. The net heat of reaction for CLOU processes is the same as CLC; only the mechanism by which oxygen is accessed by the fuel

differs. Thus, when using solid fuels like coal, the CLOU process avoids the slow gasification of the solid fuel needed to produce syngas as a prerequisite for the reaction with the oxygen carrier [10]. The oxygen carrier in CLOU must be able to release and oxidize at temperatures suitable for the process, i.e. 800 to 1200°C. This, in turn, imposes additional thermodynamic and kinetic requirements on the selected oxygen carrier.

Oxides of transition metals (Mn, Fe, Co, Ni and Cu), their mixtures, and a number of natural ores have been used as oxygen carriers in CLC [6-9]. Copper-oxide has received a great deal of attention as an efficient oxygen carrier, owing to its high reactivity, high oxygen transport capacity and absence of thermodynamic limitation for complete combustion of the fuel. Research has been conducted using copper-oxide as oxygen carrier and methane as fuel in fluidized-bed [11-15] and fixed-bed [16, 17] batch reactors, continuous operations [18-21] and thermogravimetric studies [22-25], with and without supports. Among various supports for CuO oxygen carriers, Al_2O_3 has received considerable attention [12-15, 18-20, 25, 26]. In the case of Al_2O_3 as support, a difficulty arises due to the facile interaction between CuO and Al_2O_3 either during synthesis or during operation, resulting in partial loss of CuO by formation of copper (II) aluminate ($CuAl_2O_4$) and copper (I) aluminate ($CuAlO_2$; delafossite) [14, 15, 18, 19]. However, since the copper-aluminate phases are highly reducible [13-15, 18, 19, 24, 27], the interaction between the support and the active phase does not necessarily cause a problem with respect to CLC application. For CLOU however, this interaction needs to be avoided in order to preserve CuO as active phase. Since the interaction of CuO with Al_2O_3 seems to be difficult to avoid, other supports such as TiO_2, ZrO_2, SiO_2 or $MgAl_2O_4$ likely need to be employed for CLOU [14, 18, 19, 23, 24, 28, 29].

Most of the studies mentioned above have been carried out at conditions where CuO is fully reduced to metallic Cu. It is now well known that CuO decomposes to Cu_2O when the actual concentration of oxygen is lower than the equilibrium concentration [10]. As a result, oxygen is released thereby allowing CLOU to take effect. For temperatures of 900 and 925°C, this occurs at oxygen concentrations below 1.5 and 2.7%, respectively [10]. Thus, from a CLOU point of view, the optimum temperature of the air reactor is likely in the range of 900 to 925°C. Some studies have also investigated the use of CuO oxygen carriers for combustion of solid fuels [10, 26, 28-30].

In cognizance of the potential of copper-based systems as CLOU materials, samples of CuO supported on zirconia (ZrO_2) and partially stabilized with calcia (CaO), magnesia (MgO) and ceria (CeO_2) were synthesized to assess their suitability as CLOU oxygen carriers. By changing the experimental process variables, such as reaction time and temperature, their tendencies towards the loss of active CuO phase due to the redox operation, agglomeration and defluidization were analyzed.

2. Experimental

2.1. Preparation and manufacturing of oxygen carriers

The physical properties and characteristics of the oxygen carriers used in this investigation are summarized in Table 1. The particles were manufactured by freeze-granulation. Here, a water-based slurry of CuO and inert support powders with ratio of 40/60 wt. % along with small amount of dispersant (Dolapix PC21) is prepared. The mixture is then ball milled for 24 h and a binder (Polyvinyl Alcohol) is added prior to granulation. The slurry is pumped through a spray nozzle and into liquid nitrogen to form spherical particles upon instantaneous freezing. The material is then freeze-dried at a temperature corresponding to the vapour pressure of water at -10°C. This was followed by calcination at 950 and 1050°C for 6 h at a ramp rate of 5°C min^{-1}. The calcined materials were sieved through stainless steel screens to yield particles in the range of 125-180 μm.

Table 1 Physical properties and characteristics of the oxygen carriers used in this work

Sample	Calcination Temp. [°C]	Active phase, 40 wt. %	Support phase, 60 wt. %	Crushing Strength [N]	Effective Density [g/cm^3]	BET [m^2/g]
C4MZ-950			Mg-ZrO_2 (MSZ-8 Mandoval)	0.12	1.1	1.4
C4CeZ-950	950		Ce-ZrO_2 (CEZ-10 Mandoval)	0.05	2.7	3.7
C4CaZ-950			Ca-ZrO_2 (Zirox)	0.18	1.9	0.6
		CuO				
C4MZ-1050			Mg-ZrO_2 (MSZ-8 Mandoval)	0.33	1.5	0.7
C4CeZ-1050	1050		Ce-ZrO_2 (CEZ-10 Mandoval)	0.07	3.3	1.2
C4CaZ-1050			Ca-ZrO_2 (Zirox)	0.18	1.5	0.4

2.2. Characterization of oxygen carriers

The oxygen carrier was analyzed before and after the experiments using powder X-ray diffraction (Siemens, D5000 Diffractometer) with CuK_α radiation. The morphological investigation was carried out with an environmental scanning electron microscope (ESEM) fitted with a field emission gun (FEI, Quanta 200). The BET surface area of the particles was evaluated by N_2-absorption (Micromeritics, TriStar 3000). The effective density of the particles, sized 125-180 μm was measured assuming a theoretical void fraction of 0.37 of a packed-bed with uniform spherical particles. The crushing strength of the particles was measured as the strength needed to fracture a single particle sized within 180-250 μm. An average of 30 tests per sample was obtained using a digital force gauge (Shimpo, FGN-5). The crushing strength was found to be less than 0.5 N. Although as will be shown later in Section 3, the low crushing strength did not cause any problem with respect to agglomeration or fragmentation of particles. Nonetheless for use in a full scale plant, the crushing strength would need to be increased, e.g. by optimizing the manufacturing technique.

2.3. Experimental setup and procedure

Experiments were carried out in a quartz fluidized-bed reactor, 870 mm long and 22 mm in inner diameter. A porous quartz plate was placed at a height of 370 mm from the bottom and the reactor temperature was measured with chromel-alumel (type K) thermocouples sheathed in inconel-600 located about 5 mm below and 25 mm above the plate. Honeywell pressure transducers with a frequency of 20 Hz were used to measure pressure drop over the bed in order to determine if the bed was fluidized or not. The exit gas stream from the reactor was led into a condenser to remove the water. The composition and flow rate of the dry gas was determined on a volumetric base by a Rosemount NGA-2000 analyzer which measured the concentrations of O_2, CO_2, CO, CH_4 and H_2. The schematic of the experimental setup used in this investigation is shown in Fig. 2.

A sample of 15 g was placed on the porous plate inside the fluidized-bed reactor and the bed was exposed to alternating oxidizing and reducing conditions. Prior to the test, the reactor was heated to 900°C in a stream of 5% O_2 to ensure that the oxygen carrier was in fully oxidized state. The use of 5% O_2 stream during the oxidation phase is to examine whether the oxygen carrier can be oxidized in an oxygen deficient condition similar

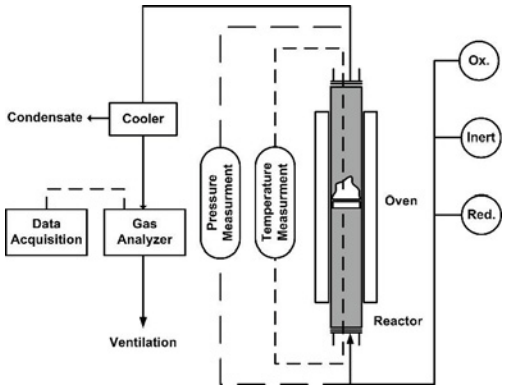

Fig. 2 Scheme of the experimental setup used in this investigation

to the outlet of the air reactor in a realistic CLOU system. A set of three inert gas cycles were initially carried out for all samples in N_2 to investigate the release of oxygen during a span of 360 s.

For reactivity test, methane was primarily used for 20 s during reduction cycles and repeated for at least three times. The duration of 20 s was selected as it approximately corresponds to the reduction of CuO to Cu_2O, assuming complete gas conversion. Subsequently, additional cycles were carried out in which the reduction time was increased in steps of 10 s intervals up to 70 s. During the prolonged reduction cycles, it is likely that reduction to Cu is gradually approached, i.e. applicable to CLC. The extended reduction time also helped in evaluating the extent to which the active CuO phase was available. There was no carbon burn-off during the subsequent oxidation cycles (indicated by way of increase in CO and/or CO_2 concentrations) to show carbon deposition during shorter reduction cycles. This was due to the fact that more oxygen was available than the stoichiometric demand of the fuel. Depending on the oxygen ratio of the respective sample, some carbon was deposited during the extended reduction cycles as they were depleted of oxygen. Nitrogen was used as an inert purge for 60 s in between oxidation and reduction. The exit gas stream from the reactor was led into a condenser to remove the water. The composition and flow rate of the dry gas was determined on a volumetric base by a Rosemount NGA-2000 analyzer which measured the concentrations of O_2, CO_2, CO, CH_4 and H_2. Inlet flow rates of 450, 900 and 600 $mL_N\ min^{-1}$ were used during reduction, oxidation and inert cycle, respectively. These flow rates were chosen to achieve values ranging between 9 to 29 u_{mf} during oxidation, 6 to 19 u_{mf} during inert and, 3 to 10 u_{mf} during reduction of the inlet flows, where u_{mf} is the minimum fluidization velocity [31].

2.4. Data analysis

The reactivity of a given oxygen carrier is quantified in terms of gas yield or conversion efficiency, γ, and is defined as the fraction of fully oxidized fuel divided by the carbon containing gases in outlet stream, in this work CO_2, CO and CH_4.

$$\gamma = \frac{y_{CO_2}}{y_{CO_2} + y_{CH_4} + y_{CO}} \tag{5}$$

Here y_i denotes the concentration (*vol.* %) of the respective gas, obtained from the gas analyzer. The mass-based conversion of the oxygen carrier, ω, is defined as

$$\omega = \frac{m}{m_{ox}} \tag{6}$$

where m and m_{ox} are respectively, the actual mass and the mass of the oxygen carrier in fully oxidized. Equations (7) and (8) are employed for calculating ω as a function of time during the reduction and oxidation period respectively from the measured concentrations of various gaseous species in the gas analyzer:

$$\omega_i = \omega_{i-1} - \int_{t_0}^{t_1} \frac{\dot{n}_{out} M_O}{m_{ox}} \left(4 y_{CO_2} + 3 y_{CO} + 2 y_{O_2} - y_{H_2}\right) dt \tag{7}$$

$$\omega_i = \omega_{i-1} + \int_{t_0}^{t_1} \frac{2 M_O}{m_{ox}} \left(\dot{n}_{in} y_{O_2,in} - \dot{n}_{out} y_{O_2,out}\right) dt \tag{8}$$

where ω_i is the instantaneous mass-based conversion at time i, ω_{i-1} the mass-based conversion in the preceding instant, t_0 and t_1 the initial and final time of measurement, M_o the molar mass of oxygen, and $\dot{n}_{out}$ the molar flow rate of dry gas at the reactor outlet.

3. Results

3.1. Concentration profiles

Fig. 3 shows the oxygen concentration during the inert gas phase following an oxidation for all samples except for the C4CaZ-950 sample which was in a powdery form and thus could not be fluidized. During this period, CuO decomposes spontaneously into Cu_2O in the environment of inert nitrogen where the particles release oxygen. The oxygen concentration is relatively consistent with the theoretical equilibrium partial pressure, p_{O_2}, corresponding to the decomposition of CuO into Cu_2O (1.5% and 2.7% respectively at 900 and 925°C [10]).

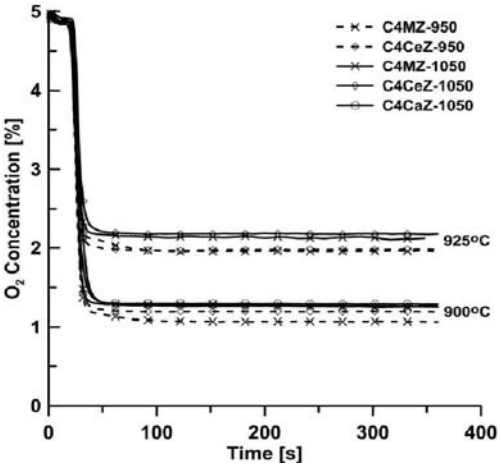

Fig. 3 Oxygen concentrations during inert gas cycles at 900 and 925°C

Following the inert gas cycles, successful cycles of oxidation and reduction were carried out for the remaining oxygen carriers, with the exception being the C4CaZ-1050 sample which experienced defluidization and agglomeration after operation at 900°C and thus the experiment had to be stopped. As an example, Fig. 4 shows the concentration profile for the C4MZ-950 sample for the third reduction cycle at 900°C. During the short interval in inert gas prior to fuel injection, the spontaneous release of oxygen via the CLOU mechanism can be seen. The fuel (methane) reacts exothermically with the released oxygen, producing CO_2, with concomitant increase in temperature due to the exothermic nature of the reaction; this is common for copper-based oxygen carriers [5]. The rise in temperature shifts the thermodynamic equilibria and in turn increases the oxygen concentration. However, the actual oxygen concentration during reduction in the reactor is lower due to dilution created by the water formed. This water is removed in the cooler prior to the gas analyzer. Note that no CH_4 or CO was detected during the entire reducing period, and hence full gas yield was clearly achieved. The concentration profiles were similar from cycle to cycle, except for slight variations in peak concentrations due to the transitory non-steady state. At 925°C, more oxygen is released during the inert and reduction cycles.

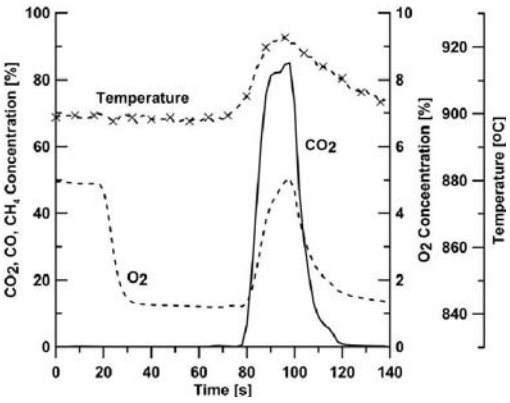

Fig. 4 Concentration and temperature profiles for C4MZ-950 during reduction for 20 s using CH_4 at 900°C

3.2. Reactivity of oxygen carriers

Fig. 5 shows the reactivity (in terms of gas yield, γ) of the C4MZ and C4CeZ oxygen carriers at 925°C, using methane as fuel for the third repeated cycle. The point at which γ plummets indicates the end of 20 s of reduction. Except for C4CeZ-1050, the remaining samples exhibited high reactivity with complete fuel conversion during this period. Similar results were obtained for reactivity tests at 900°C.

The carriers lose approximately 3% of their mass as they are converted during 20 s of reduction (ω going from 1 to 0.97) which is also consistent with the expected mass loss. The C4CeZ-1050 sample however does not comply with the reactivity shown by the other samples. This will be further examined in the following.

Fig. 6 shows the oxygen partial pressure as a function of oxygen carrier conversion, ω, in the oxidation phase following the reduction cycle at 900°C for the C4MZ and C4CeZ samples. Note that in Fig. 5 approximately 3% mass-based conversion of the oxygen carriers was reached during 20 s of reduction, i.e. ω going from 1 to 0.97. Thus during the oxidation cycle that follows, the carrier is expected to retrieve the amount of oxygen withdrawn from the carrier, meaning that ω must revert from 0.97 to 1. Only then, a truly reversible redox behavior of the carrier is achieved. For the C4MZ samples as shown in Fig. 6, the carriers retrieve the expected conversion with the value of ω extending to 1 at the equilibrium oxygen concentration (approximately 1.5%) for all oxidation cycles and irrespective of the calcination temperature. This shows that the active CuO phase has likely remained intact in the C4MZ samples. However, it can be conceived for the C4CeZ-950 and C4CeZ-1050 samples that the oxygen partial pressure follows the equilibrium concentration at 1.5% and rises to 5%, long before full conversion of the oxygen carrier is achieved. The incomplete retrieval of ω in the C4CeZ materials indicate that part of the active CuO phase is not restored upon oxidation. This explains the incomplete conversion of the fuel during the subsequent reduction cycles for the C4CeZ-1050 sample, as shown in Fig. 5. Although this did not cause any deficiency in the C4CeZ-950 oxygen carrier for conversion of methane during the 20 s reduction cycles (Fig. 5), the deficiency in active CuO phase becomes also more evident for this oxygen carrier as discussed in the following.

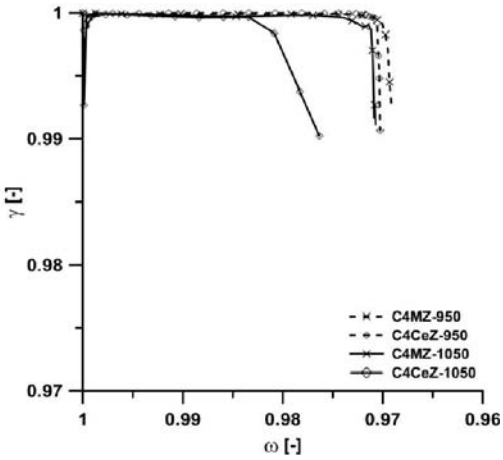

Fig. 5 Gas yield, γ, as a function of mass-based conversion, ω, for C4MZ and C4CeZ oxygen carriers during 20 s of CH_4 reduction at 925°C

Fig. 7 shows the gas yield (γ) for the C4MZ and C4CeZ samples at 925°C during the extended reduction cycle (70 s) with methane. Under the experimental conditions and the oxygen carriers employed, the theoretical conversion of CuO to Cu, ω, at the end of reduction should correspond to 0.92. This was nearly obtained only in the case of C4MZ-950 where ω reaches a value of 0.93 with full conversion of methane. This confirms that the limit of CuO reduction to Cu is reached. On the contrary, in the case of C4MZ-1050 and in the case of C4CeZ samples a lower value of ω is reached. This indicates that the C4CeZ oxygen carriers did not oxidize completely in the oxidation cycles prior to the reduction as described above and as shown in Fig. 6. Although it was possible to oxidize the C4MZ-1050 oxygen carrier in the previous oxidization cycles (Fig. 6), the reactivity in the prolonged reduction cycle (70 s) does

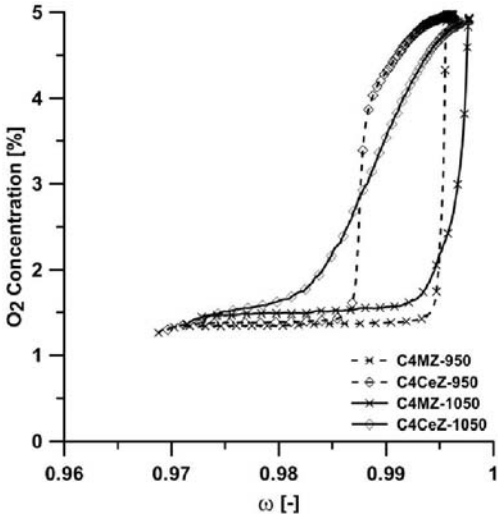

Fig. 6 Variation of oxygen concentration with mass-based conversion (ω) during oxidation at 900°C for C4MZ and C4CeZ oxygen carriers

not comply with the intact content of active CuO phase as seen in the case of C4MZ-950 (Fig. 7).

From the reactivity test shown in Fig. 5-7, it can be inferred that among investigated oxygen carriers, only C4MZ-950 exhibits a relatively intact active CuO phase. This is true for both oxidizing and reducing experiments in the temperature regime of investigation. The C4MZ-1050 and C4CeZ samples however did not show an intact active CuO phase after the several cycles carried out in the reactivity test. Thus the loss of active CuO phase in these oxygen carries (Fig. 6 and 7) raises questions about their long-term stability as CLOU materials. The characterization of the oxygen carriers in Section 3.3 discusses the observed difficulty in case of the C4CeZ and C4MZ-1050 samples in more detail.

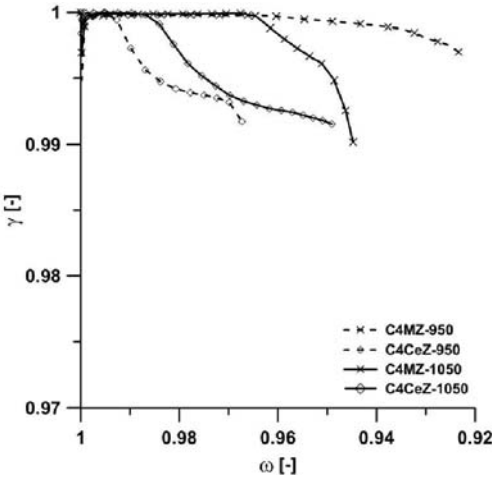

Fig. 7 Gas yield (γ) as a function of mass-based conversion (ω) for C4MZ and C4CeZ oxygen carriers at 925°C during 70 s of CH_4 reduction

3.3. Physical aspects of the oxygen carriers under redox cycle

Physical characteristics of the fresh oxygen carriers were given in Table 1. The BET surface areas of the used samples did not show any significant variation; the observed small change could be within the experimental error. Table 2 shows the XRD characterization of all fresh and tested samples. The experiments were always ended in the oxidation phase and thus the characterization of the used samples refers to this phase. For the C4MZ-950 oxygen carrier, the fresh and used particles had identical XRD patterns also confirming the intactness of the active CuO phase in these particles. However, in case of the C4MZ-1050 and C4CeZ samples, Cu_2O was found in the used samples, indicating that these oxygen carriers were not fully oxidized to CuO.

Table 2 XRD characterization of the oxygen carriers used in this work

Sample	Fresh	After reactivity testing
C4MZ-950	CuO, $Mg_{0.857}Cu_{2.143}O_3$*, ZrO_2	CuO, $Mg_{0.857}Cu_{2.143}O_3$*, ZrO_2
C4CeZ-950	CuO, $Ce_{0.05}Zr_{0.95}O_2$, $Ce_{0.97}Zr_{0.03}O_2$*, ZrO_2*	CuO, Cu_2O, $Ce_{0.05}Zr_{0.95}O_2$, $Ce_{0.97}Zr_{0.03}O_2$*
C4CaZ-950	CuO, $Ca_{0.15}Zr_{0.85}O_{1.85}$, ZrO_2	---
C4MZ-1050	CuO, $(Mg_{0.88}Cu_{0.12})Cu_2O_3$*, ZrO_2	CuO, Cu_2O,$(Mg_{0.88}Cu_{0.12})Cu_2O_3$*, ZrO_2
C4CeZ-1050	CuO, $Ce_{0.02}Zr_{0.98}O_2$, $Ce_{0.75}Zr_{0.25}O_2$*	CuO, Cu_2O, $Ce_{0.02}Zr_{0.98}O_2$, $Ce_{0.75}Zr_{0.25}O_2$*
C4CaZ-1050	CuO, $Ca_{0.15}Zr_{0.85}O_{1.85}$, ZrO_2	---

* Minor phase

It is reported that the diffusion of O_2 in the depleted oxygen carrier in the oxidation cycle could be hindered by the CuO layer partially surrounding the reduced Cu_2O and Cu grains [32]. Therefore the incomplete oxidation of the C4MZ-1050 and C4CeZ samples could be connected with this resistance. However, such behaviour was not seen in case of the C4MZ-950 sample, as ω was completely restored during the subsequent oxidation phases.

The ESEM images of fresh and post reaction for C4CMZ and C4CeZ oxygen carriers are shown in Fig. 8 (a-h). It can be observed for the C4MZ-950 sample, Fig. 8 (a-b), that the oxygen carrier particles remain individual with insignificant morphology change and no observable fragmentation or agglomeration. This in fact shows the stability and thermal resistivity of this oxygen carrier. For the C4MZ-1050 oxygen carrier however, agglomeration of the particles is evident in Fig. 8 (d). This could

also account for the lower reactivity seen during the prolonged reduction cycles (Fig. 7) as the material sinters during the redox cycles. The ESEM images of the C4CeZ materials, Fig. 8 (e-h) shows similarities before and after the reactivity test in surface morphologies, however with formation of fines which may also account for the loss of the active CuO phase in these oxygen carries (Fig. 6 and 7). From the foregoing set of observations, it can be inferred that the C4MZ-950 material is a suitable oxygen carrier for the CLOU process. This is corroborated by the invariant amount of active CuO phase (Fig. 6 and 7) and absence of agglomeration and particle fragmentation as seen in Fig. 8 (a-b) for this material.

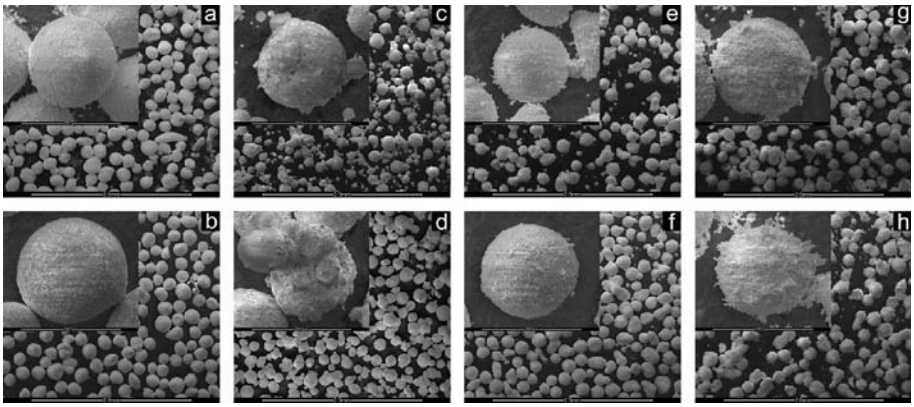

Fig. 8 Fresh (upper row) and post reaction (bottom row) ESEM images of (a-b) C4MZ-950 and (c-d) C4MZ-1050, (e-f) C4CeZ-950 and (g-h) C4CeZ-1050 oxygen carriers

4. Conclusions

The use of CuO oxygen carriers supported on magnesia (MgO), calcia (CaO) and ceria (CeO_2) stabilized zirconia (ZrO_2) as CLOU materials have been investigated. The oxygen carriers were calcined at 950 and 1050^{o}C. Five out of the six materials investigated showed the rapid release of oxygen in an inert environment (CLOU). Also, complete conversion of methane during 20 s of exposure was obtained for three out of the six materials. In case of the MgO-stabilized ZrO_2 as support and calcined at 950^{o}C, the active CuO phase remained intact and no agglomeration or defluidization tendencies were observed. Hence, the use of this material could be suggested as a suitable oxygen carrier for the CLOU process, although long-term validation of its use with in continuous operation is needed.

Acknowledgements

The authors wish to thank Vattenfall and Chalmers University of Technology via the Energy Area of Advance for the financial support of this work.

References

[1] R.K. Pachauri, A. Reisinger, *Fourth Assesment Report: Climate Change (Synthesis Report)*, Intergovernmental Panel on Climate Change, Geneva, 2007.
[2] A. Lyngfelt, B. Leckner, T. Mattisson, A fluidized-bed combustion process with inherent CO_2 separation; application of chemical-looping combustion, *Chem. Eng. Sci.* 2001;**56**:3101-3113.
[3] M. Ishida, H. Jin, A Novel Chemical-Looping Combustor without NO_x Formation, *Ind. Eng. Chem. Res.* 1996;**35**:2469-2472.
[4] B. Kronberger, E. Johansson, G. Löffler, T. Mattisson, A. Lyngfelt, H. Hofbauer, A Two-Compartment Fluidized Bed Reactor for CO_2 Capture by Chemical-Looping Combustion, *Chem. Eng. Technol.* 2004;**27**:1318-1326.

[5] E. Jerndal, T. Mattisson, A. Lyngfelt, Thermal Analysis of Chemical-Looping Combustion, *Chem. Eng. Res. Des.* 2006;**84**:795-806.
[6] A. Lyngfelt, Oxygen Carriers for Chemical Looping Combustion - 4000 h of Operational Experience, *Oil Gas Sci. Technol.* 2011;**66**:161-172
[7] A. Lyngfelt, T. Mattisson, *Materials for chemical-looping combustion*, WILEY-VCH Verlag GmbH & Co. KGaA, Weinheim, 2011.
[8] M.M. Hossain, H.I. de Lasa, Chemical-looping combustion (CLC) for inherent CO_2 separations-a review, *Chem. Eng. Sci.* 2008;**63**:4433-4451.
[9] J. Adanez, A. Abad, F. Garcia-Labiano, P. Gayan, L.F. de Diego, Progress in Chemical-Looping Combustion and Reforming technologies, *Progr. Energy Combust. Sci.* 2012;**38**:215-282.
[10] T. Mattisson, A. Lyngfelt, H. Leion, Chemical-looping with oxygen uncoupling for combustion of solid fuels, *Int. J. Greenhouse Gas Control* 2009;**3**:11-19.
[11] P. Cho, T. Mattisson, A. Lyngfelt, Comparison of iron-, nickel-, copper- and manganese-based oxygen carriers for chemical-looping combustion, *Fuel* 2004;**83**:1215-1225.
[12] L.F. de Diego, P. Gayán, F. García-Labiano, J. Celaya, A. Abad, J. Adánez, Impregnated CuO/Al_2O_3 Oxygen Carriers for Chemical-Looping Combustion: Avoiding Fluidized Bed Agglomeration, *Energy Fuels* 2005;**19**:1850-1856.
[13] S.Y. Chuang, J.S. Dennis, A.N. Hayhurst, S.A. Scott, Development and performance of Cu-based oxygen carriers for chemical-looping combustion, *Combust. Flame* 2008;**154**:109-121.
[14] M. Arjmand, A.-M. Azad, H. Leion, A. Lyngfelt, T. Mattisson, Prospects of Al_2O_3 and $MgAl_2O_4$-Supported CuO Oxygen Carriers in Chemical-Looping Combustion (CLC) and Chemical-Looping with Oxygen Uncoupling (CLOU), *Energy Fuels* 2011;**25**:5493-5502.
[15] M. Arjmand, A.-M. Azad, H. Leion, A. Lyngfelt, T. Mattisson, Evaluation of $CuAl_2O_4$ as an Oxygen Carrier in Chemical-looping Combustion (CLC), *Ind. Eng. Chem. Res.* 2012;DOI: 10.1021/ie300427w.
[16] B.M. Corbella, L. De Diego, F. García, J. Adánez, J.M. Palacios, The Performance in a Fixed Bed Reactor of Copper-Based Oxides on Titania as Oxygen Carriers for Chemical Looping Combustion of Methane, *Energy Fuels* 2005;**19**:433-441.
[17] B.M. Corbella, L. de Diego, F. García-Labiano, J. Adánez, J.M. Palacios, Characterization and Performance in a Multicycle Test in a Fixed-Bed Reactor of Silica-Supported Copper Oxide as Oxygen Carrier for Chemical-Looping Combustion of Methane, *Energy Fuels* 2005;**20**:148-154.
[18] P. Gayán, C.R. Forero, A. Abad, L.F. de Diego, F. García-Labiano, J. Adánez, Effect of Support on the Behavior of Cu-Based Oxygen Carriers during Long-Term CLC Operation at Temperatures above 1073 K, *Energy Fuels* 2011;**25**:1316–1326.
[19] C.R. Forero, P. Gayán, F. García-Labiano, L.F. de Diego, A. Abad, J. Adánez, High temperature behaviour of a $CuO/\gamma Al_2O_3$ oxygen carrier for chemical-looping combustion, *Int. J. Greenhouse Gas Control* 2011;**5**:659-667.
[20] L.F. de Diego, F. García-Labiano, P. Gayán, J. Celaya, J.M. Palacios, J. Adánez, Operation of a 10 kWth chemical-looping combustor during 200 h with a $CuO\text{-}Al_2O_3$ oxygen carrier, *Fuel* 2007;**86**:1036-1045.
[21] J. Adánez, P. Gayán, J. Celaya, L.F. de Diego, F. García-Labiano, A. Abad, Chemical Looping Combustion in a 10 kW_{th} Prototype Using a CuO/Al_2O_3 Oxygen Carrier: Effect of Operating Conditions on Methane Combustion, *Ind. Eng. Chem. Res.* 2006;**45**:6075-6080.
[22] Q. Zafar, T. Mattisson, B. Gevert, Redox Investigation of Some Oxides of Transition-State Metals Ni, Cu, Fe, and Mn Supported on SiO_2 and $MgAl_2O_4$, *Energy Fuels* 2005;**20**:34-44.
[23] J. Adánez, L.F. de Diego, F. García-Labiano, P. Gayán, A. Abad, J.M. Palacios, Selection of Oxygen Carriers for Chemical-Looping Combustion, *Energy Fuels* 2004;**18**:371-377.
[24] L.F. de Diego, F. GarcIa-Labiano, J. Adánez, P. Gayán, A. Abad, B.M. Corbella, J. MarIa Palacios, Development of Cu-based oxygen carriers for chemical-looping combustion, *Fuel* 2004;**83**:1749-1757.
[25] T. Mattisson, A. Järdnäs, A. Lyngfelt, Reactivity of Some Metal Oxides Supported on Alumina with Alternating Methane and OxygenApplication for Chemical-Looping Combustion, *Energy Fuels* 2003;**17**:643-651.
[26] J.S. Dennis, C.R. Müller, S.A. Scott, In situ gasification and CO_2 separation using chemical looping with a Cu-based oxygen carrier: Performance with bituminous coals, *Fuel* 2010;**89**:2353-2364.
[27] S.Y. Chuang, J.S. Dennis, A.N. Hayhurst, S.A. Scott, Kinetics of the chemical looping oxidation of H_2 by a co-precipitated mixture of CuO and Al_2O_3, *Chem. Eng. Res. Des.* 2011;**89**:1511-1523.
[28] T. Mattisson, H. Leion, A. Lyngfelt, Chemical-looping with oxygen uncoupling using CuO/ZrO_2 with petroleum coke, *Fuel* 2009;**88**:683-690.
[29] M. Arjmand, M. Keller, H. Leion, A. Lyngfelt, M. Mattisson, Oxygen Release and Oxidation Rates of $MgAl_2O_4$-Supported CuO in a Fluidized-bed Reactor for Chemical-looping Combustion with Oxygen Uncoupling (CLOU), *Energy Fuels* 2012;DOI: 10.1021/ef3010064.
[30] A. Abad, I. Adánez-Rubio, P. Gayán, F. García-Labiano, L.F. de Diego, J. Adánez, Demonstration of chemical-looping with oxygen uncoupling (CLOU) process in a 1.5kW_{th} continuously operating unit using a Cu-based oxygen-carrier, *Int. J. Greenhouse Gas Control* 2012;**6**:189-200.
[31] D. Kunni, O. Levenspiel, *Fluidization Engineering*, Butterworth-Heinemann, Stoneham, 1991.
[32] S.Y. Chuang, J.S. Dennis, A.N. Hayhurst, S.A. Scott, Kinetics of the Oxidation of a Co-precipitated Mixture of Cu and Al_2O_3 by O_2 for Chemical-Looping Combustion, *Energy Fuels* 2010;**24**:3917-3927.